ARTICLE
Journal of Cellular Biochemistry 114:2160–2169 (2013)

Journal of Cellular Biochemistry

MiR-23a in Amplified 19p13.13 Loci Targets Metallothionein 2A and Promotes Growth in Gastric Cancer Cells

Juan An,[1,2] Yuanming Pan,[1] Zhi Yan,[1] Wenmei Li,[1] Jiantao Cui,[1] Jiao Yuan,[3] Liqing Tian,[3] Rui Xing,[1*] and Youyong Lu[1*]

[1]*Laboratory of Molecular Oncology, Key Laboratory of Carcinogenesis and Translational Research (Ministry of Education), Peking University Cancer Hospital/Institute, Beijing, 100142, P.R., China*

[2]*High Altitude Medical Research Center, Department of Basic Medical Sciences, Qinghai University, Xining, Qinghai Province, 810001, P.R., China*

[3]*Laboratory of Bioinformatics and Noncoding RNA, Institute of Biophysics, Chinese Academy of Sciences, Beijing, 100101, P.R., China*

ABSTRACT

Copy number variation (CNV) and abnormal expression of microRNAs (miRNAs) always lead to deregulation of genes in cancer, including gastric cancer (GC). However, little is known about how CNVs affect the expression of miRNAs. By integrating CNV and miRNA profiles in the same samples, we identified eight miRNAs (miR-1274a, miR-196b, miR-4298, miR-181c, miR-181d, miR-23a, miR-27a and miR-24-2) that were located in the amplified regions and were upregulated in GC. In particular, amplification of miR-23a-27a-24-2 cluster and miR-181c-181d cluster frequently occurred at 19p13.13 and were confirmed by genomic real-time PCR in another 25 paired GC samples. Moreover, in situ hybridization (ISH) experiments represented that mature miR-23a was increased in GCs (75.5%, 40/53) compared with matched normal tissues (28.6%, 14/49, $P = 0.001$). Knocking down of miR-23a expression inhibited BGC823 cell growth in vitro and in vivo. In addition, the potential target genes of miR-23a were investigated by integration of mRNA profile and miRNA TargetScan predictions, we found that upregulation of miR-23a and downregulation of metallothionein 2A (MT2A) were detected simultaneously in 70% (7/10) of the miRNA and mRNA profiles. Furthermore, an inverse correlation between miR-23a and MT2A expression was detected in GCs and normal tissues. Through combining luciferase assay, we confirmed that MT2A is a potential target of miR-23a. In conclusion, these results suggest that integration of CNV-miRNA-mRNA profiling is a powerful tool for identifying molecular signatures, and that miR-23a might play a role in regulating MT2A expression in GC. J. Cell. Biochem. 114: 2160–2169, 2013.

KEY WORDS: miR-23a; GASTRIC CANCER; COPY NUMBER VARIATION; MT2A

Genomic profiling and high-throughput cancer transcriptome microarrays have uncovered genetic alterations that drive tumorigenesis and tumor progression [Pinkel and Albertson, 2005; Ting et al., 2006]. Chromosomal instability is a characteristic of cancer [Ushijima, 2005] including GC [Vauhkonen et al., 2006; Yang et al., 2007]. These aberrations lead to critical deregulation of gene expression and function [Santarius et al., 2010]. Recently, genome-wide CNV studies have identified dozens of CNV-associated protein-coding genes, which aid the identification of molecular signatures that can act as predictive and prognostic markers for cancers [Stranger et al., 2007; Conrad et al., 2010]. However, little is known about CNVs of small non-coding RNAs, particularly miRNAs in GC.

MiRNAs are ~20-nt non-coding RNAs that are implicated in the regulation of diverse biological pathways [Ambros, 2004]. A number

Juan An and Yuanming Pan contributed equally to this work.

Grant sponsor: The National High Technology Research and Development Program of China (863 Program); Grant numbers: 2006AA02A402, 2012AA02A504; Grant sponsor: The National Basic Research Program of China (973 Program); Grant number: 2004CB518708.

*Correspondence to: Dr. Youyong Lu and Rui Xing, Laboratory of Molecular Oncology, Key Laboratory of Carcinogenesis and Translational Research (Ministry of Education), Peking University Cancer Hospital/Institute, 52 Fu-Cheng Road, Haidian District, Beijing 100142, P.R. China. E-mail: youyonglu@hsc.pku.edu.cn; sherry19820420@hotmail.com

Manuscript Received: 2 November 2012; Manuscript Accepted: 28 March 2013

Accepted manuscript online in Wiley Online Library (wileyonlinelibrary.com): 4 April 2013

DOI 10.1002/jcb.24565 • © 2013 Wiley Periodicals, Inc.

of miRNAs are dysregulated in carcinogenesis, and specific miRNAs that regulate proliferation, invasion and metastasis have been identified [Lu et al., 2005; Esquela-Kerscher and Slack, 2006; Manikandan et al., 2008]. Several studies have shown that miRNA expression can be modified by CNV [Ota et al., 2004; He et al., 2005; Zhang et al., 2006]. CNV-miRNAs (copy number variation-associated miRNAs) potentially have altered function and should be considered as high priority candidates for research into genotype–phenotype association in cancer [Marcinkowska et al., 2011].

In this study, we used three types of microarrays from the same set of 20 paired GC specimens to study genetic variation in DNA, miRNA and mRNA, including CNV profile, miRNA array, and mRNA expression profiles (data not shown). Our goal was to determine molecular signatures in GC using a high-throughput combined profiling strategy and to find out how GC-specific variations contribute to GC. We identified GC-associated miRNAs by adopting a combined CNV-miRNA analysis, and candidate targets of these miRNAs were identified by integration of gene expression profiling data. In addition, we attempted to establish a link between the genotype and the phenotype by integration of CNV-miRNA-mRNA profiles in GC. Furthermore, the biological role of abnormally expressed miRNA in GC was studied.

MATERIALS AND METHODS

BIOINFORMATICS

Significant analysis of microarrays (SAM) was used to perform the unsupervised clustering calculation. We chose a fold change greater than 1, and $q < 0.05$ as the selection criteria for the differential expression of miRNAs. The Cluster and Treeview programs were used to perform hierarchical clustering of miRNA genes. A *t*-test was performed to evaluate the significance of differential expressed miRNAs in miRNA arrays. Moreover, the sLDA algorithm [Wu et al., 2009] was used to detect differentially expressed miRNAs. We assigned miRNA genes to CNV sites, using the Sanger miRNA database 4.0 (http://www.mirbase.org/) and the UCSC genome browser database (http://genome.ucsc.edu/).The miRNA targets predicted by Target Scan 5.0 (http://www.targetscan.org/) were integrated with the gene profiling from paired GC samples.

QUANTITATIVE REAL-TIME PCR AND IN SITU HYBRIDIZATION

Genomic DNA was isolated using the QIAamp DNA Mini Kit (Qiagen, Valencia, CA). RNA was extracted from cells using a standard Trizol protocol (Invitrogen, Life Technologies, Grand Island, NY). Mature miRNA sequences were acquired from the Sanger institute miRBase sequence database. Real-time PCR analyses were performed with SYBR Premix Ex Taq (TaKaRa, Japan). The primers used are shown in the supplemental information (Supplementary Table SII).

The miR-23a probe had the sequence GGAAATCCCTGGCAATGTGAT (predicted T_m: 54°C, measured T_m: 62°C; miRCURY™ probe, Exiqon, Vedbaek, Denmark). A U6 probe (sequence: CACGAATTTGCGTGTCATCCTT, predicted T_m: 75°C, measured T_m: 65°C, Exiqon) was used as the positive control and a 22-mer scrambled probe with a random sequence was included as a negative control (GTGTAACACGTCTATACGCCCA, predicted T_m: 78°C, measured ™:65°C Exiqon). All locked nucleic acid (LNA) oligos were digoxigenin (DIG)-labeled at the 5′ and 3′ ends, except for the U6 probe. In situ hybridization (ISH) was then performed using miRCURY LNA™ microRNA ISH Optimization Kit (Exiqon).

CELL LINES, CONSTRUCTION OF PLASMIDS, AND RNA INTERFERENCE

Human GC cell lines, BGC823, MGC803, AGS, and GES1 (a human immortal gastric epithelial cell line) were maintained in Dulbecco′s modified Eagle′s medium (DMEM, GIBCO-BRL, Life Technologies) with 5% FBS. To generate stable Ps-miR-23a or vector-transfected BGC823 cell lines, transfection was performed using Lipofectamine 2000 (Invitrogen). Forty-eight hours after transfection, the transfected cells were incubated for 3 weeks in DMEM with 400 μg/ml of G418 (Genview, IL, USA). Successful and stable transfection of Ps-miR-23a into BGC823 cells was confirmed by quantitative reverse transcription PCR (qRT-PCR).

We amplified a fragment containing the miR-23a precursor from genomic DNA. The amplified fragment was cloned into a pcDNA3.1 and was termed as Pc-miR-23a. To construct 3′ UTR reporter plasmids, 3′ UTR fragments of MT2A mRNA, containing the putative miR-23a binding site, were cloned into *Bgl*II/*Hin*dIII sites in the pGL3.0-reporter plasmid (Promega, USA). Knockdown of miR-23a was investigated in BGC823 cells by small hairpin RNA (shRNA) analysis. MiR-23a-3p mimics and miR-23a-3p mutation were synthesized and purified by RiboBio (RiboBio Co. Ltd, Guangzhou, China). RNA oligonucleotides were transfected using Lipofectamine RNAi-MAX (Invitrogen) and the medium was replaced 6 h after transfection. RNA transfection efficiency was approximately 70–80% and ectopic expression of the miRNA or knockdown of miRNA expression persisted for at least 48 h. All oligonucleotide sequences are listed in Supplementary Table SII.

MTT AND COLONY FORMATION ASSAY

Cell proliferation was determined by the 3-(4,5-dimethylthiazol-2-Yl)-2,5-diphenyltetrazolium bromide (MTT) assay (Sigma, St. Louis, MO). BGC823 cells were seeded in 96-well plates with 2×10^3 cells per well in 100 μl of cell culture medium and incubated at 37°C for 24 h. The cells were then transfected with Ps-miR-23a or empty vector. After incubation for 1–6 days, the cells were incubated with 20 μl of MTT (at a final concentration of 0.5 mg/ml) at 37°C for 4 h. The absorbance at 570 nm was detected using a Quant Universal Microplate Spectrophotometer (Bio-tek Instruments, Winooski, VT).

BGC823 cells were seeded at 1,000 cells per well in 6-well plates. Cells were transfected with Ps-miR-23a or empty vector. Twenty-four hours after transfection, the medium was replaced with fresh medium containing G418. Plates were incubated at 37°C in a 5% CO_2 humidified atmosphere for 3 weeks. Once colonies were visible, they were stained with methylene blue and photographed.

TUMORIGENICITY IN NUDE MICE

All experimental procedures involving animals were performed in accordance with the Guide for the Care and Use of Laboratory Animals (NIH publications Nos. 80-23, revised 1996) and were according to the institutional ethical guidelines for animal experiments. Four-week-old female Balb/c nude mice were used for

tumorigenicity analysis. The tumorigenicity of stable Ps-miR-23a or vector-transfected BGC823 cells was measured. 5×10^5 cells in 0.1 ml PBS were injected subcutaneously into nude mice. Tumor growth was measured 5 days after injection and every 5 days thereafter. Tumor volume (V) was monitored by measuring the length (L) and width (W) with calipers and calculated using the formula $(L \times W^2) \times 0.5$.

DUAL-LUCIFERASE REPORTER GENE ASSAY

Ps-miR-23a-1 + 3′ UTR-pGL3.0 MT2A reporter, Ps-miR-23a-2 + 3′ UTR pGL3.0 MT2A reporter, or Ps-vector + 3′ UTR-pGL3.0 MT2A reporter were co-transfected into BGC823 cells. In addition, the luciferase activity in GES1 cells transfected with miR-23a-3p mimics + 3′ UTR-pGL3.0 MT2A reporter and miR-23a-3p mutation + 3′ UTR-pGL3.0 MT2A reporter was assayed. The luciferase reporter gene assay was performed using the Dual-Luciferase Reporter Assay System (Promega). All experiments were performed at least three times.

WESTERN BLOTTING AND IMMUNOFLUORESCENCE STAINING

BGC823 cells were transfected with Ps-miR-23a-1, Ps-miR-23a-2 or vector. Western blotting was performed using Western Blotting Detection Reagents (Amersham Biosciences, Buckinghamshire, UK). Immunodetection was performed using a mouse anti-human MT2A monoclonal antibody (ab12228, AbCam, Cambridge, UK) and mouse anti-human β-actin (Santa Cruz, CA). For immunofluorescence staining, cells were subsequently reacted with FITC-labeled secondary antibodies for 1 h, and nuclei were stained with DAPI (Invitrogen) for 3 min. Images of cells with a fluorescent signal were captured by laser confocal microscopy (Leica Sp5 Laser Scanning Confocal Microscope, GE).

IMMUNOHISTOCHEMISTRY (IHC)

We constructed a tissue microarray (TMA) comprising 53 human gastric specimens obtained from the tumor bank of Beijing Cancer Hospital. Hematoxylin and eosin (H&E)-stained sections were used for histological verification. Written informed consent was obtained from all the patients. IHC staining was performed using an EnVision+ Kit (Dako, Denmark). Sections were cultured with antibody against MT2A (AbCam). A positive reaction in this experiment was defined staining of more than 10% of cells in the tissue. Two pathologists who were blinded to the clinical status of patients scored the images visually.

RESULTS

IDENTIFICATION OF miRNAs BY INTEGRATING GENOMIC CNVs AND miRNA EXPRESSION PROFILING OF GC

We performed whole genome-CNV profile by Human CNV370-Duo DNA BeadChips in 20 matched GC samples (data not shown). To explore the potential miRNAs in the CNV regions, we assigned miRNAs to these regions using the UCSC genome browser database. Ninety-two miRNAs were identified in the regions showing gain or loss of DNA (Fig. 1A and Supplementary Table SI). Meanwhile, we used the SAM algorithm to identify distinct miRNA expression signatures in a miRNA microarray of 10 matched GC cases from the same samples. Forty-seven upregulated and 17 downregulated miRNAs were identified that were statistically significantly different in GC samples compared with normal tissues (Fig. 1B). Furthermore, to identify cancer-related miRNAs, we performed an integrated analysis of CNVs and miRNA expression profiles from the same group of samples. Eight miRNAs (miR-1274a, miR-196b, miR-4298, miR-181c, miR-181d, miR-23a, miR-27a, and miR-24-2) were amplified in related genomic regions and their transcripts overexpressed. The significance of overlap was confirmed by Fisher's exact test, 2.53-fold enrichment of co-localization over random chance ($P = 0.026$, Fig. 1C and Table I).

IDENTIFICATION OF miR-23a AS A PUTATIVE BIOMARKER OF GC

Among the selected miRNAs in the amplified loci, five belong to the miR-23a-27a-24-2 cluster or the miR-181c-181d cluster located at 19p13.13 (5/20, 25%), and were chosen for further study (Fig. 2A). We then carried out genomic real-time PCR in 25 matched GC samples to analyze the copy numbers of the miRNA clusters. Amplification of the miR-23a-27a-24-2 cluster and the miR-181c-181d cluster were detected in GC tissues compared with normal tissues ($P = 0.035$ and $P = 0.042$, respectively; Wilcoxon test; Fig. 2B). Furthermore, the *t*-test and sLDA algorithms were used for miRNA identification. Taking the results of the two methods into consideration, mature miR-23a, miR-196a, and miR-3172 were identified, which had low *P* values in the *t*-test, and high sLDA values, suggesting that their expression was significantly different between GCs and matched normal tissues (Fig. 2C). By combining the CNV-miRNA analysis with results from two differential algorithms, miR-23a was selected as a candidate GC miRNA. Furthermore, in situ hybridization showed that miR-23a was upregulated in 75.5% (40/53) GC tissues compared with low levels in 49 matched normal tissues 28.6% (14/49, $P = 0.001$; Fig. 2D). These results confirmed the expression of miR-23a in GC, as initially determined by miRNA expression profiling.

DOWNREGULATION OF miR-23a INHIBITS TUMOR CELL GROWTH IN VITRO AND IN VIVO

To explore the role of miR-23a in gastric tumorigenesis, knockdown of miR-23a was investigated in BGC823 cells that showed a high level of endogenous miR-23a expression. BGC823 cells were transfected with shRNA constructs Ps-miR-23a-1, Ps-miR-23a-2, and empty vector, respectively. MiR-23a expression in Ps-miR-23a-2 transfectants was significantly downregulated and was selected for further study ($P = 0.02$, Fig. 3A). The MTT assay showed that downregulation of miR-23a inhibited cell growth (Fig. 3B). Colony formation analysis showed that, compared with control cells, Ps-miR-23a cells produced fewer and smaller colonies ($P = 0.031$, Fig. 3C). Furthermore, the mean volume of Ps-miR-23a xenografts was significantly smaller than the control xenografts (Fig. 3D). These data suggest that downregulation of miR-23a inhibits cell growth in vitro and in vivo.

MT2A, THE POTENTIAL TARGET GENE OF miR-23a, IS REDUCED IN GC

We integrated the gene expression profiling data with TargetScan predictions to identify 45 putative targets of miR-23a. Among these, MT2A was selected as a better candidate target gene of miR-23a (Fig. 4A), because upregulation of miR-23a and downregulation of

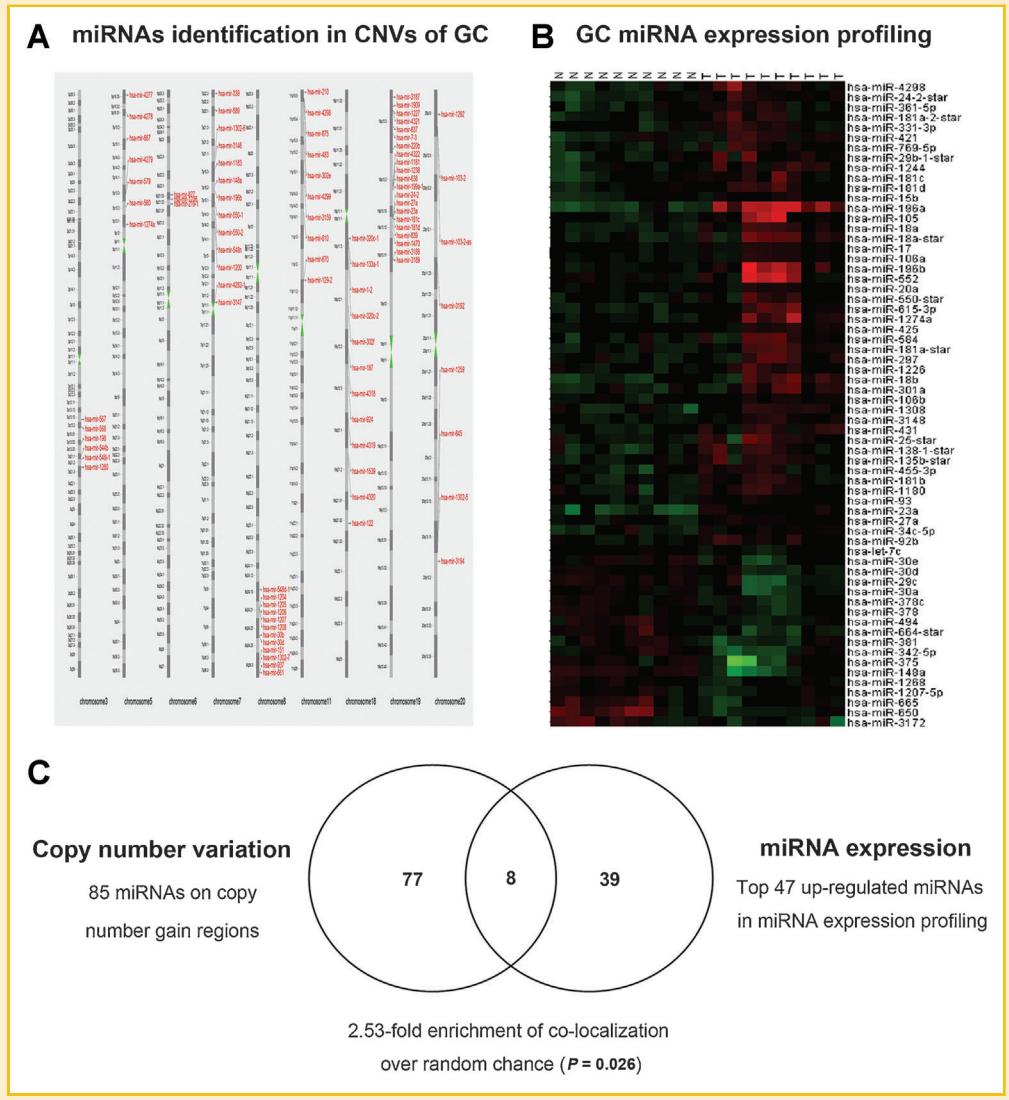

Fig. 1. Integrated analysis of CNVs and miRNA expression profiling of GC. A: Ninety-two miRNAs were identified in the amplified or deleted regions. B: Forty-seven upregulated and 17 downregulated miRNAs were identified from GC miRNA arrays. Columns represent samples and rows represent genes, which are color-coded (black, green, and red correspond to no-change, downregulated, and upregulated, respectively). C: An integrated analysis of 47 upregulated miRNAs and 85 miRNAs located in amplified regions. The Venn diagram shows eight miRNAs that were both upregulated and amplified in GC.

MT2A were detected simultaneously in 70% (7/10) of the miRNA and gene expression profiles (Fig. 4B). In GC cell lines (BGC823, MGC803, and AGS), the level of miR-23a expression was higher than in normal immortal gastric epithelial cells GES1. Conversely, MT2A was lower in GC cell lines than in GES1 (Fig. 4C). Furthermore, ISH showed that levels of miR-23a were high in 65.8% (23/35) of GC tissues compared with in 34.2% (12/35, $P = 0.008$) of matched normal tissues, while IHC analysis showed that levels of MT2A were high in 74.3% (26/35) of normal tissues, but low or absent in 25.7% (9/35, $P < 0.0001$) of GC tissues. These results showed an inverse correlation between mature

TABLE I. Identification of Significant miRNA in Amplified Regions

miRNA ID	Chromosome	Region	CNV region position	Positive case total 20 (%)
miR-1274a	chr 5	p15.33–p12	73747–46384240	6 (30%)
miR-196b	chr 7	p22.3–p11.1	37124–58032993	5 (25%)
miR-4298	chr11	p15.5–p11.2	348027–45633399	7 (35%)
miR-181c	chr19	p13.3–p13.11	233753–18883204	5 (25%)
miR-181d	chr19	p13.3–p13.11	233753–18883204	5 (25%)
miR-23a	chr19	p13.3–p13.11	233753–18883204	5 (25%)
miR-27a	chr19	p13.3–p13.11	233753–18883204	5 (25%)
miR-24-2	chr19	p13.3–p13.11	233753–18883204	5 (25%)

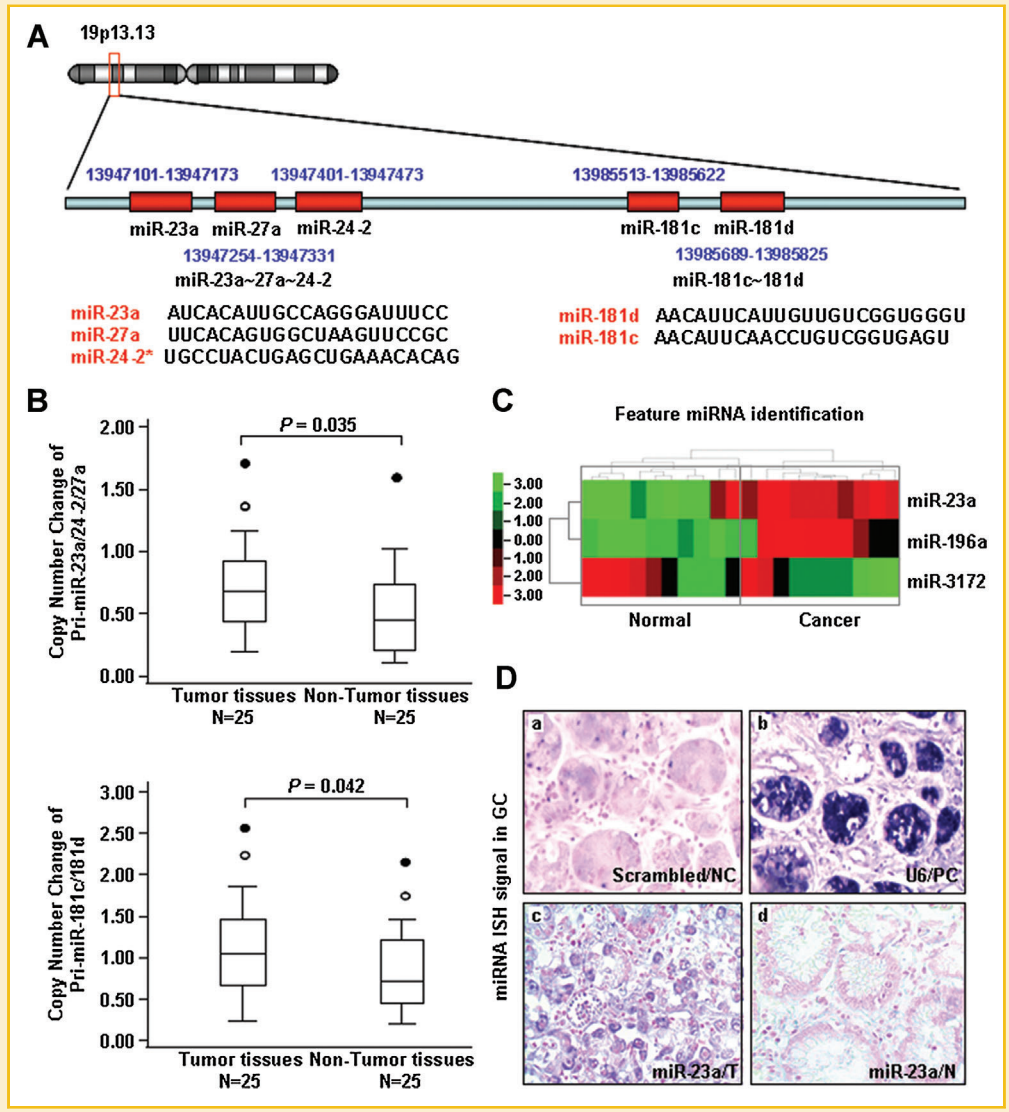

Fig. 2. Identification of miR-23a as a putative biomarker of GC. A: Schematic diagram of the sequences and genomic loci of miR-23a, miR-27a, miR-24-2, miR-181c, and miR-181d at 19p13.13. B: The genomic copies of the miR-23a-27a-24-2 cluster and miR-181c-181d cluster in 25 GC tissues compared with matched normal tissues was performed by real-time PCR. Fucose-1-phosphate guanylyltransferase (FPGT) was used for normalization. The copy number change of miRNAs was calculated using the $2^{-\Delta\Delta C_T}$ method. C: A heat map displaying alterations of miRNAs' expressions in gastric tumors and normal tissues. Columns represent samples and rows represent genes, which are color-coded (black, green, and red correspond to no-change, downregulated, and upregulated, respectively). D: The expression level of miR-23a detected by in situ hybridization. Tissue sections were obtained from 53 gastric tumors and 49 normal tissues. a: DIG-labeled LNA scrambled sequence probe was used as negative control (NC). b: DIG-labeled LNA snRNA U6 probe were used as the positive control (PC). c: High level of miR-23a expression in 75.5% (40/53) of gastric tumors. d: MiR-23a was expressed at a low level or not all in 71.4% (35/49) of normal tissues ($P = 0.001$).

miR-23a and MT2A expression in GC tissues and matched normal tissues ($P = 0.026$, Spearman's correlation coefficient $R = -0.401$; Fig. 4D).

miR-23a REGULATES MT2A EXPRESSION IN GC CELLS

We further analyzed the effect of miR-23a on the downregulation of MT2A expression. RT-PCR and Western blotting demonstrated upregulation of MT2A expression in BGC823 cells transfected with Ps-miR-23a-1 and Ps-miR-23a-2 compared with vector-transfected cells. Confocal analysis showed that MT2A protein levels were higher in BGC823 cells transfected with Ps-miR-23a-1 and Ps-miR-23a-2 than in vector-transfected cells (Fig. 5A). Tumor sections from xenografts were obtained and analyzed by ISH and IHC staining. MT2A was detected in the ps-miR-23a-transfectant tumors, but not in control tumors (Fig. 5B). To further confirm the possibility that miR-23a targets MT2A, a dual-luciferase reporter system was employed. BGC823 cells were cotransfected with Ps-miR-23a-1/2 + 3′ UTR-pGL3.0 MT2A reporter, as well as Ps-vector + 3′ UTR-pGL3.0 MT2A reporter. The relative luciferase activity in Ps-miR-23a-1/2 + 3′ UTR-pGL3.0 MT2A reporter cotransfected groups was significantly higher than that of the Ps-vector + 3′ UTR-pGL3.0 MT2A reporter group (Fig. 5C). In addition, overexpression of miR-23a in GES1 cells greatly reduced MT2A protein and mRNA expression levels (Fig. 5D–E). Moreover, the luciferase activity in GES1 cells transfected with miR-

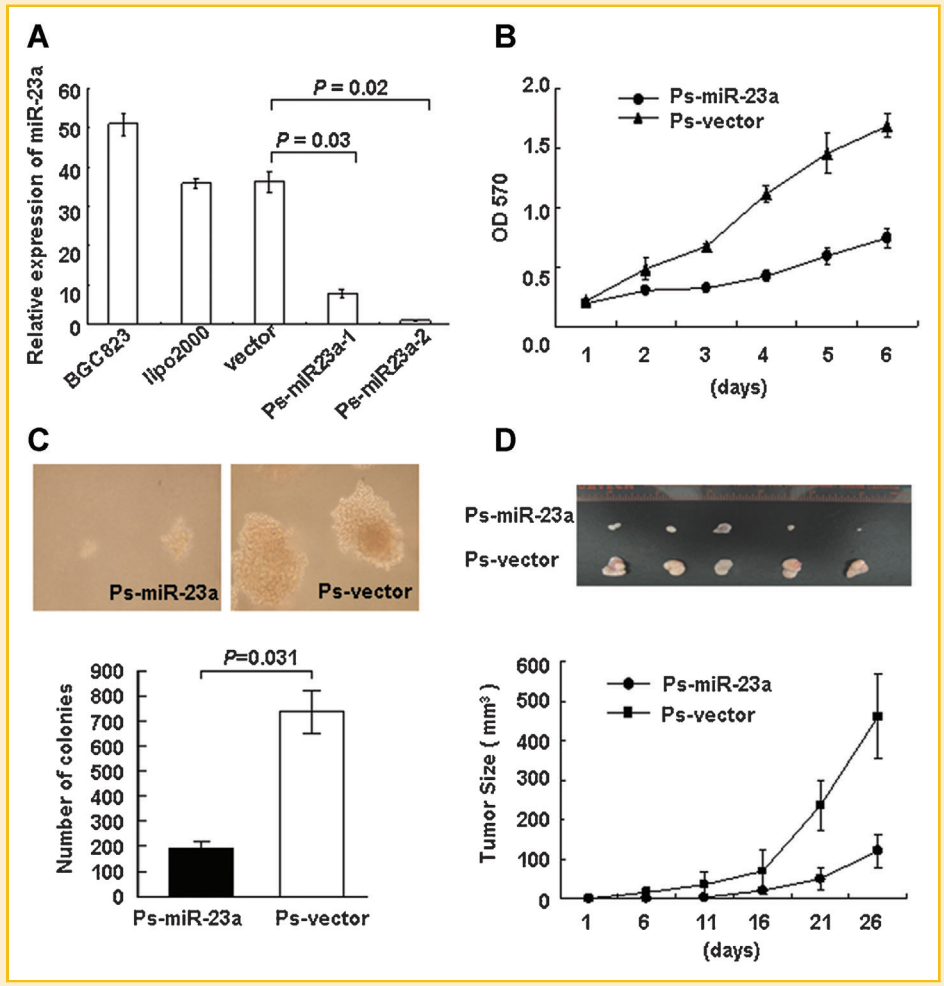

Fig. 3. Depletion of miR-23a inhibits cancer cell growth in vitro and in vivo. A: Relative level of miR-23a expression in BGC823 cells after transfection with Ps-miR-23a-1, Ps-miR-23a-2, or empty vector. Significant downregulation of miR-23a was detected by qRT-PCR in BGC823 cells transfected with Ps-miR-23a-1 and Ps-miR-23a-2. B: Cell growth was detected using the MTT assay. Growth inhibition was detected in Ps-miR-23a-transfected cells compared with vector-transfected cells at different time periods. Data are the mean ± SD from three independent experiments. C: Ps-miR-23a-transfected cell colonies were smaller than the vector-transfected cell colonies when grown on soft agar. Fewer Ps-miR-23a-transfected cell colonies were detected in soft agar compared with vector-transfected cell colonies. D: Downregulation of miR-23a inhibits xenograft tumor formation of GC cells. The xenografts of Ps-miR-23a-transfected cells produced significantly smaller tumors than the vector-transfected xenografts. The average size of tumors developed in nude mice is shown as the mean ± SE.

23a mimics + 3′ UTR-pGL3.0 MT2A reporter was significantly suppressed compared with miR-23a mutation + 3′ UTR-pGL3.0 MT2A reporter transfected cells ($P = 0.018$, Fig. 5F). These data suggested that MT2A is a potential target of miR-23a.

DISCUSSION

Chromosomal aberrations are frequently observed in GC, but little is known about functional non-coding sequences, particularly miRNAs, at the CNV regions in GC. Here, we present a systematic array-based survey of combined CNV-miRNA-mRNA profiles that aimed to establish a link between genotype and phenotype and to identify molecular signatures in GC (Supplementary Fig. 1). Our integrative analysis included data from high resolution CNV profiles, miRNA arrays, and mRNAs expression profiles in GC. By integrated analysis of CNV-miRNA profiles from the same set of GC samples, eight upregulated miRNAs (miR-1274a, miR-196b, miR-4298, miR-181c, miR-181d, miR-23a, miR-27a, and miR-24-2) were identified in amplified regions. Among these, five miRNAs (the miR-23a-27a-24-2 cluster, and the miR-181c-181d cluster) were located in amplified region of 19p13.13, and were confirmed by genomic real-time PCR. MiR-23a was selected for further study and high levels of miR-23a were observed in primary GCs compared with that in normal controls. Importantly, overexpression of miR-23a promoted BGC823 cell growth by downregulating MT2A expression as its potential target, based on mRNA expression profiling of GC.

CNVs can influence the expression of genes [Iafrate et al., 2004; Perry et al., 2007]. However, few studies have assessed the role of CNVs on miRNA expression, and many miRNAs that are located in fragile genomic sites or aberrant regions are associated with cancer

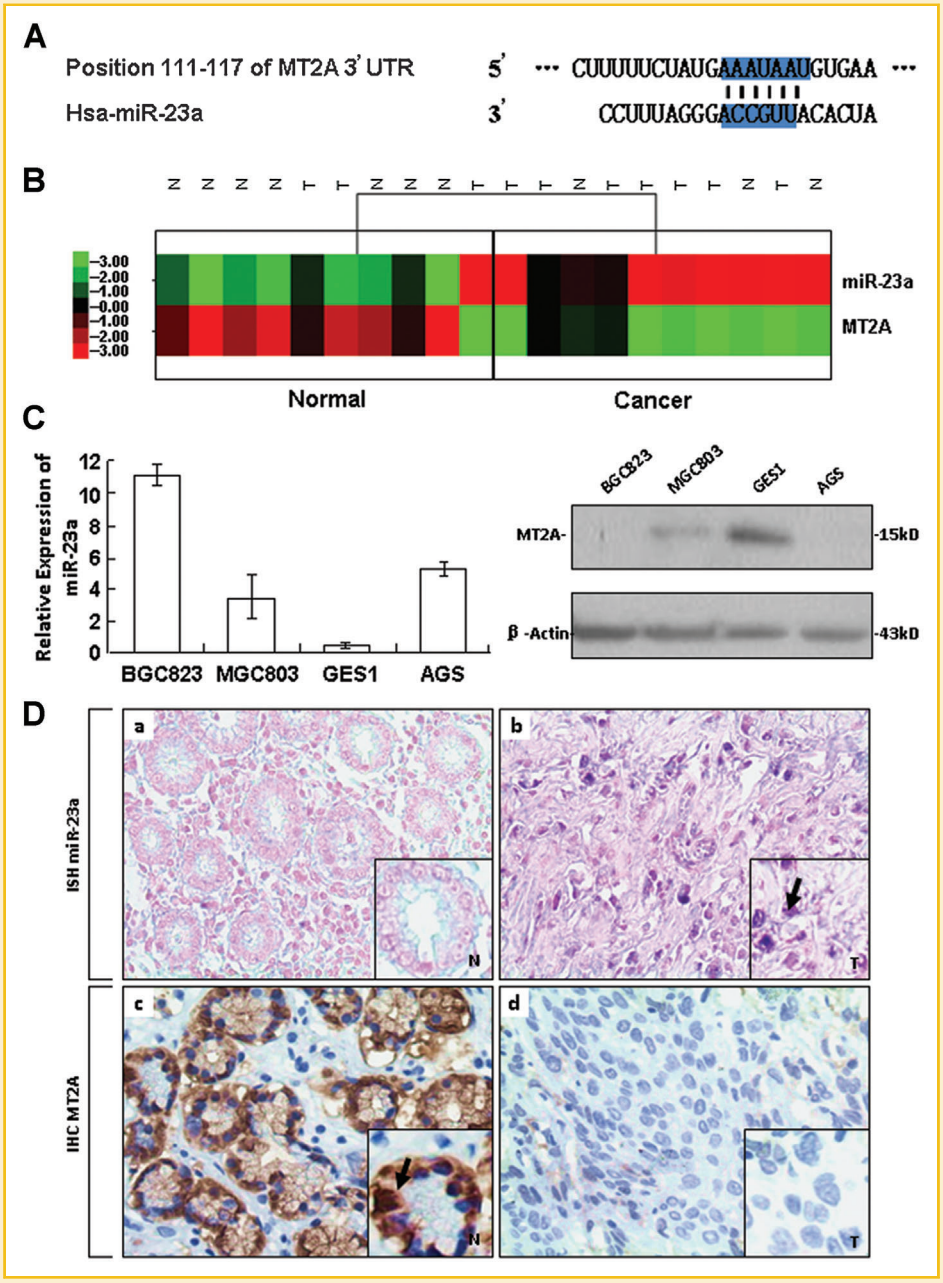

Fig. 4. Correlation analysis of miR-23a and MT2A expression in cell lines and primary GC tumors. A: The binding sites of miR-23a sequences in the 3′ UTR of the MT2A gene. B: Cluster analysis of miR-23a and MT2A expression patterns in GC miRNA and mRNA profiling data. Upregulation of miR-23a and downregulation of MT2A were detected simultaneously in the same samples (7/10). C: Differential expression of miR-23a and MT2A in four tumor cell lines detected by qRT-PCR and Western blotting, respectively. The levels of miR-23a and MT2A inversely correlated in gastric cell lines. D ISH and IHC were used to detect the expression patterns of miR-23a and MT2A in GCs and matched normal tissues, respectively. a: Decreased or absent miR-23a expression was detected in normal tissues. b: miR-23a was highly expressed in GCs. c: MT2A was highly expressed in normal tissues. d: Decreased or absent MT2A expression was detected in GCs.

[Calin et al., 2004]. Meanwhile, cancer genetics studies supported the view that CNVs affect the expression of miRNAs [Marcinkowska et al., 2011]. CNV-miRNAs are involved in many processes and phenotypes, including organ development, angiogenesis, and tumorigenesis [Marcinkowska et al., 2011].

Copy number amplification of 19p13 has been detected in many cancers, such as ovarian carcinoma [Micci et al., 2010], nasopharyngeal carcinoma [Or et al., 2010], gastric carcinoma [Morohara et al., 2006], and intracranial pediatric ependymoma [Pezzolo et al., 2008]. According to previous reports, upregulation of the miR-23a-27a-24-2 cluster induces cell proliferation [Huang et al., 2008; Chhabra et al., 2010] and decreased transforming growth factor-beta-induced tumor-suppression in human hepatocellular carcinoma [Huang et al., 2008]. In MGC803 cells, a gastric cancer cell line, miR-23a promoted cell growth by downregulating the interleukin-6 receptor [Zhu et al., 2010].

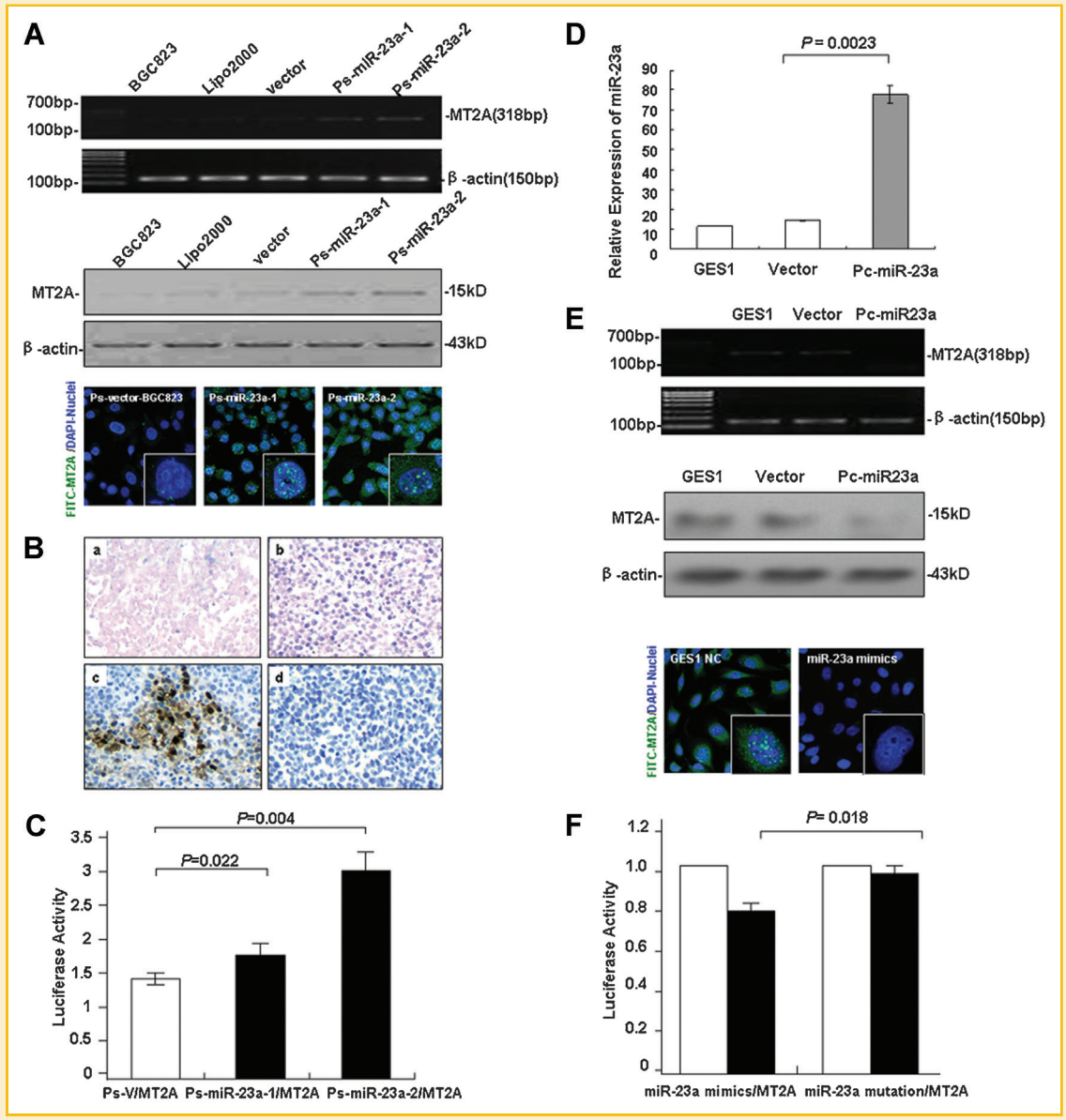

Fig. 5. MT2A is regulated by miR-23a in GC cells. A: High expression levels of MT2A were detected in BGC823 cells transfected with Ps-miR-23a-1 and Ps-miR-23a-2 relative to vector-transfected cells by RT-PCR (upper), Western blotting (middle), and immunofluorescence analysis (lower). B: ISH and IHC were performed on tissue sections obtained from nude mice tumor tissues. a: miR-23a was not expressed in nude mice tumor tissues derived from Ps-miR-23a transfectants; (b) Overexpression of miR-23a was detected in vector transfectants; (c) MT2A was detected in nude mice tumor tissues derived from Ps-miR-23a transfectants; and (d) MT2A was not expressed in vector-transfected tissues. C: The relative luciferase activity in Ps-miR-23a-1/2 + 3′ UTR-pGL3.0 MT2A reporter cotransfected groups were significantly higher than that of the empty vector + 3′ UTR-pGL3.0 MT2A reporter group. D: GES1 cells were transfected with either Pc-miR-23a or vector. The expression of miR-23a was detected by real-time PCR in GES1 cells transfected with Pc-miR-23a. E: Significant downregulation of MT2A was detected by RT-PCR (upper), Western blotting (middle), and immunofluorescence analysis (lower) in GES1 cells transfected with Pc-miR-23a. F: The relative luciferase activity was significantly suppressed in GES1 cells when cotransfected with miR-23a mimics + 3′ UTR-pGL3.0 MT2A reporter. No suppression of expression was observed in the miR-23a mutant + 3′ UTR-pGL3.0 MT2A reporter group.

To investigate the mechanism of miR-23a promotion of GC cells′ growth, we identified its potential target genes. By predicting target genes using TargetScan and integrating these results with the GC mRNA expression profiles from the same group of samples, MT2A was identified as a target of miR-23a. Expression of MT2A is frequently downregulated in GC [Janssen et al., 2000; Kim et al., 2005] and MT2A inhibits cell proliferation by inducing cell apoptosis [Janssen et al., 2000; Cui et al., 2003]. We showed an inverse correlation between miR-23a expression and MT2A expression in GC cells and tissues. Further data suggested that MT2A is a potential target of miR-23a.

Our study provides a combined model of CNV-miRNA-mRNA profiles in GC. This model could provide a potential bridge from genotype to phenotype. Amplified miRNA clusters in 19p13.13 may be associated with the development of GC. Especially, overexpression of miR-23a from this region leads to down-regulation of MT2A and

proliferation of GC cells (Supplementary Fig. 2). These results represent potential genetic biomarkers that could lead to improved techniques for the diagnosis and prognosis of GC patients.

ACKNOWLEDGMENTS

We are grateful to Prof. Runsheng Chen for help with the analysis of biological information, Prof. Xianghong Li for reviewing hematoxylin and eosin-stained samples, and the Tissue Bank of Beijing Cancer Hospital for gastric specimens.

REFERENCES

Ambros V. 2004. The functions of animal microRNAs. Nature 431:350–355.

Calin GA, Sevignani C, Dumitru CD, Hyslop T, Noch E, Yendamuri S, Shimizu M, Rattan S, Bullrich F, Negrini M, Croce CM. 2004. Human microRNA genes are frequently located at fragile sites and genomic regions involved in cancers. Proc Natl Acad Sci USA 101:2999–3004.

Chhabra R, Dubey R, Saini N. 2010. Cooperative and individualistic functions of the microRNAs in the miR-23a-27a-24-2 cluster and its implication in human diseases. Mol Cancer 9:232.

Conrad DF, Pinto D, Redon R, Feuk L, Gokcumen O, Zhang Y, Aerts J, Andrews TD, Barnes C, Campbell P, Fitzgerald T, Hu M, Ihm CH, Kristiansson K, Macarthur DG, Macdonald JR, Onyiah I, Pang AW, Robson S, Stirrups K, Valsesia A, Walter K, Wei J, Tyler-Smith C, Carter NP, Lee C, Scherer SW, Hurles ME. 2010. Origins and functional impact of copy number variation in the human genome. Nature 464:704–712.

Cui Y, Wang J, Zhang X, Lang R, Bi M, Guo L, Lu SH. 2003. ECRG2, a novel candidate of tumor suppressor gene in the esophageal carcinoma, interacts directly with metallothionein 2A and links to apoptosis. Biochem Biophys Res Commun 302:904–915.

Esquela-Kerscher A, Slack FJ. 2006. Oncomirs—microRNAs with a role in cancer. Nat Rev Cancer 6:259–269.

He L, Thomson JM, Hemann MT, Hernando-Monge E, Mu D, Goodson S, Powers S, Cordon-Cardo C, Lowe SW, Hannon GJ, Hammond SM. 2005. A microRNA polycistron as a potential human oncogene. Nature 435:828–833.

Huang S, He X, Ding J, Liang L, Zhao Y, Zhang Z, Yao X, Pan Z, Zhang P, Li J, Wan D, Gu J. 2008. Upregulation of miR-23a approximately 27a approximately 24 decreases transforming growth factor-beta-induced tumor-suppressive activities in human hepatocellular carcinoma cells. Int J Cancer 123:972–978.

Iafrate AJ, Feuk L, Rivera MN, Listewnik ML, Donahoe PK, Qi Y, Scherer SW, Lee C. 2004. Detection of large-scale variation in the human genome. Nat Genet 36:949–951.

Janssen AM, van Duijn W, Oostendorp-Van DRM, Kruidenier L, Bosman CB, Griffioen G, Lamers CB, van Krieken JH, van De Velde CJ, Verspaget HW. 2000. Metallothionein in human gastrointestinal cancer. J Pathol 192:293–300.

Kim JM, Sohn HY, Yoon SY, Oh JH, Yang JO, Kim JH, Song KS, Rho SM, Yoo HS, Kim YS, Kim JG, Kim NS. 2005. Identification of gastric cancer-related genes using a cDNA microarray containing novel expressed sequence tags expressed in gastric cancer cells. Clin Cancer Res 11:473–482.

Lu J, Getz G, Miska EA, Alvarez-Saavedra E, Lamb J, Peck D, Sweet-Cordero A, Ebert BL, Mak RH, Ferrando AA, Downing JR, Jacks T, Horvitz HR, Golub TR. 2005. MicroRNA expression profiles classify human cancers. Nature 435:834–838.

Manikandan J, Aarthi JJ, Kumar SD, Pushparaj PN. 2008. Oncomirs: The potential role of non-coding microRNAs in understanding cancer. Bioinformation 2:330–334.

Marcinkowska M, Szymanski M, Krzyzosiak WJ, Kozlowski P. 2011. Copy number variation of microRNA genes in the human genome. BMC Genomics 12:183.

Micci F, Skotheim RI, Haugom L, Weimer J, Eibak AM, Abeler VM, Trope CG, Arnold N, Lothe RA, Heim S. 2010. Array-CGH analysis of microdissected chromosome 19 markers in ovarian carcinoma identifies candidate target genes. Genes Chromosomes Cancer 49:1046–1053.

Morohara K, Tajima Y, Nakao K, Nishino N, Aoki S, Kato M, Sakamoto M, Yamazaki K, Kaetsu T, Suzuki S, Tsunoda A, Tachikawa T, Kusano M. 2006. Gastric and intestinal phenotypic cell marker expressions in gastric differentiated-type carcinomas: Association with E-cadherin expression and chromosomal changes. J Cancer Res Clin Oncol 132:363–375.

Or YY, Chung GT, To KF, Chow C, Choy KW, Tong CY, Leung AW, Hui AB, Tsao SW, Ng HK, Yip TT, Busson P, Lo KW. 2010. Identification of a novel 12p13.3 amplicon in nasopharyngeal carcinoma. J Pathol 220:97–107.

Ota A, Tagawa H, Karnan S, Tsuzuki S, Karpas A, Kira S, Yoshida Y, Seto M. 2004. Identification and characterization of a novel gene, C13orf25, as a target for 13q31–q32 amplification in malignant lymphoma. Cancer Res 64:3087–3095.

Perry GH, Dominy NJ, Claw KG, Lee AS, Fiegler H, Redon R, Werner J, Villanea FA, Mountain JL, Misra R, Carter NP, Lee C, Stone AC. 2007. Diet and the evolution of human amylase gene copy number variation. Nat Genet 39:1256–1260.

Pezzolo A, Capra V, Raso A, Morandi F, Parodi F, Gambini C, Nozza P, Giangaspero F, Cama A, Pistoia V, Garre ML. 2008. Identification of novel chromosomal abnormalities and prognostic cytogenetics markers in intracranial pediatric ependymoma. Cancer Lett 261:235–243.

Pinkel D, Albertson DG. 2005. Array comparative genomic hybridization and its applications in cancer. Nat Genet 37(Suppl):S11–S17.

Santarius T, Shipley J, Brewer D, Stratton MR, Cooper CS. 2010. A census of amplified and overexpressed human cancer genes. Nat Rev Cancer 10: 59–64.

Stranger BE, Forrest MS, Dunning M, Ingle CE, Beazley C, Thorne N, Redon R, Bird CP, de Grassi A, Lee C, Tyler-Smith C, Carter N, Scherer SW, Tavare S, Deloukas P, Hurles ME, Dermitzakis ET. 2007. Relative impact of nucleotide and copy number variation on gene expression phenotypes. Science 315:848–853.

Ting AH, McGarvey KM, Baylin SB. 2006. The cancer epigenome—Components and functional correlates. Genes Dev 20:3215–3231.

Ushijima T. 2005. Detection and interpretation of altered methylation patterns in cancer cells. Nat Rev Cancer 5:223–231.

Vauhkonen H, Vauhkonen M, Sajantila A, Sipponen P, Knuutila S. 2006. DNA copy number aberrations in intestinal-type gastric cancer revealed by array-based comparative genomic hybridization. Cancer Genet Cytogenet 167:150–154.

Wu MC, Zhang L, Wang Z, Christiani DC, Lin X. 2009. Sparse linear discriminant analysis for simultaneous testing for the significance of a gene set/pathway and gene selection. Bioinformatics 25:1145–1151.

Yang S, Jeung HC, Jeong HJ, Choi YH, Kim JE, Jung JJ, Rha SY, Yang WI, Chung HC. 2007. Identification of genes with correlated patterns of variations in DNA copy number and gene expression level in gastric cancer. Genomics 89:451–459.

Zhang L, Huang J, Yang N, Greshock J, Megraw MS, Giannakakis A, Liang S, Naylor TL, Barchetti A, Ward MR, Yao G, Medina A, O'Brien-Jenkins A, Katsaros D, Hatzigeorgiou A, Gimotty PA, Weber BL, Coukos G. 2006. microRNAs exhibit high frequency genomic alterations in human cancer. Proc Natl Acad Sci USA 103:9136–9141.

Zhu LH, Liu T, Tang H, Tian RQ, Su C, Liu M, Li X. 2010. MicroRNA-23a promotes the growth of gastric adenocarcinoma cell line MGC803 and downregulates interleukin-6 receptor. FEBS J 277:3726–3734.

SUPPORTING INFORMATION

Additional supporting information may be found in the online version of this article at the publisher's web-site.

Supplementary Figure 1. Row chart describing the steps involved in the study.

Supplementary Figure 2. Proposed model of miR-23a targeting MT2A in GC cells. Upregulation of miRNA genes clustered in 19p13.13 may be associated with GC development. Genomic amplification of miR-23a results in high levels of miR-23a expression in GC cells and tissues. In addition, miR-23a could promote cell growth through the target gene, MT2A.

Supplementary Table SI. Common miRNAs in Genome-Wide CNV Regions of GC.

Supplementary Table SII. The Primer Sequences.